01,14

Atomistic simulation of grain boundary sliding in bicrystals of the CoNiCrFeMn alloy

© I.N. Karkin, L.E. Karkina, Yu.N. Gornostyrev

M.N. Mikheev Institute of Metal Physics, Ural Branch, Russian Academy of Sciences, Yekaterinburg, Russia

E-mail: lidiakarkina@gmail.com

Received June 7, 2025
Revised July 19, 2025
Accepted July 20, 2025

The influence of grain-boundary segregations in the equiatomic high-entropy CoNiCrFeMn alloy (HEA) when annealing within the range of the moderate temperatures on grain boundary sliding is studied using atomistic simulation. It is shown that in the solid-solution state during grain boundary sliding the alloy behaves qualitatively similarly to a pure FCC metal. Formation of a segregation layer on the grain boundaries during annealing has a multidirectional effect on mechanisms of sliding along special grain boundaries of an inclination $\Sigma 5$. The influence of HEA annealing on stability of an ensemble of grain boundaries is discussed.

Keywords: high-entropy alloys, segregations, grain boundaries, atomistic simulation, grain boundary sliding.

DOI: 10.61011/PSS.2025.08.62250.159-25

1. Introduction

Doping is one of the most important methods of increasing structural stability and improving mechanical properties of metals. Grain-boundary segregations that are formed during thermal-mechanical treatment of materials can significantly decrease mobility of grain boundaries (GB), increasing thermal stability of a grain structure. The review [1] considers the main types of distribution of doped atoms near the grain boundaries: complexones (single-layer, multi-layer and amorphous interlayers) [2,3] and ordered distribution of impurity atoms near the grain boundaries — grain-boundary superstructures. The type of the originating grain-boundary superstructure is determined by many factors: a boundary type (special or of a general type; symmetrical or asymmetrical), specific features of interaction of one impurity atoms with a selected grain boundary; external conditions (the temperature, the concentration of a dopant, etc.). During MD/MC simulation of annealing of the doped Al alloys, which includes atom exchange in the Monte Carlo (MC) scheme and relaxation of their positions by the molecular dynamics (MD) method, we have shown that it was possible to reconstruct a structure of grain boundaries, which was initiated by the grain-boundary superstructure being formed [4–6].

Another situation is realized in the high-entropy alloys (HEA) which are a multi-component solid solution close to a equiatomic solution. Thus, it is found during MD/MC simulation of the HEA CoNiCrFeMn bicrystal that an early stage of annealing forms short-range order regions that are uniformly distributed in the volume and contain the atoms Fe-Co or Ni-Mn-Cr [7,8]. With increase of the annealing time, redistribution of the atoms of various sorts between the GB region and the grain volume becomes dominant. There is a pronounced tendency to formation of segregations at the grain boundaries, wherein the main segregating element is Cr, whose concentration at the grain boundaries can be 35−45 at.%. As a result, unusually wide (of about 20 Å) segregations in the form of closely spaced clusters are formed at the grain boundaries. In some cases, we obtain structural reconstruction of the region near the grain boundaries, which is initiated not by formation of the grain-boundary superstructure (as in lightly doped alloys), but by significant concentration heterogeneity near the grain boundaries of the atoms that make up the HEA.

Grain boundary sliding (GB sliding) and migration of the grain boundaries are processes that along with intragranular sliding and process of accommodation in triple junctions provide plastic deformation of polycrystalline materials. Presently, atomistic simulation has been used to fairly well study the influence of the grain-boundary superstructure on the mechanisms of sliding and fracture along the grain boundaries, which are especially relevant in nanograin materials. Several specific mechanisms of grain-boundary deformation for pure metals are identified, namely, combined sliding and migration of the grain boundaries, which are defined by a geometry of special symmetrical grain boundaries [9–11]. It is shown for asymmetrical special boundaries that lattice dislocations can easily slide transversely into a closely-packed plane that forms the asymmetrical grain boundary [10]. The influence of the segregations on variation of the grain boundary sliding mechanisms is studied for the symmetrical grain boundaries [9]. In our studies [9,10] we have investigated the influence of the grain-boundary superstructure on sliding along the grain boundaries $\Sigma 5\{013\}\langle 100\rangle$ and $\Sigma 5\{012\}\langle 100\rangle$ in the alloys Al−3 at.% Mg and Al−3 at.% Ni. It is shown

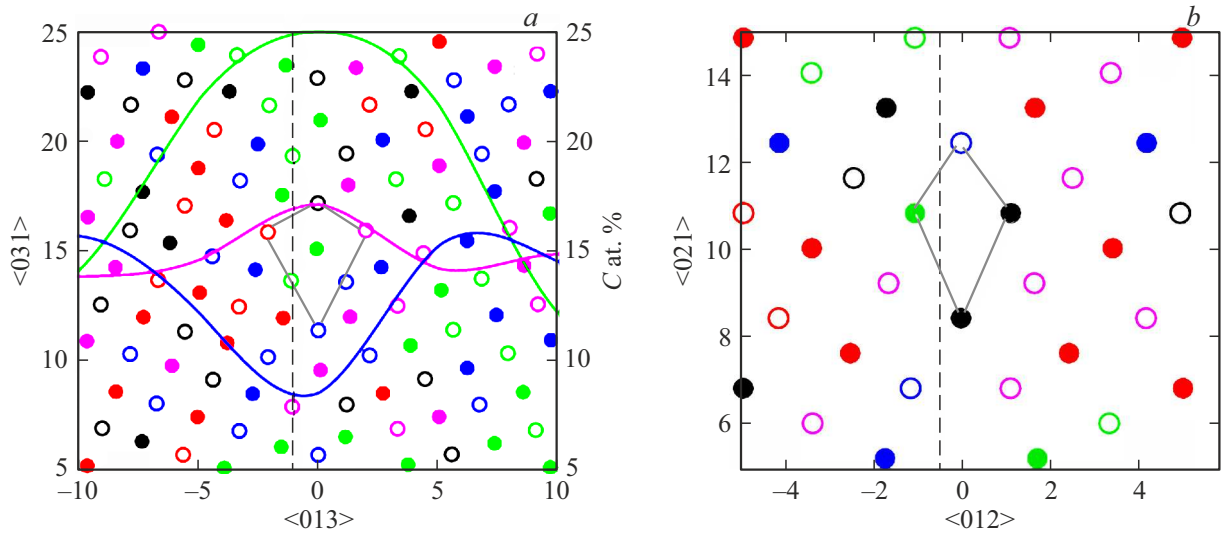

Figure 1. Fragments of starting configurations of the bicrystals with the grain boundaries $\Sigma5\{013\}\langle100\rangle$ (*a*) and $\Sigma5\{012\}\langle100\rangle$ (*b*). The gray lines mark structure units, while the hatched and unhatched circles mark atoms in two adjacent planes $\{100\}$ that are perpendicular to a boundary inclination axis. The thin solid lines mark distribution of the concentration after annealing. The black dots correspond to Co, the blue dots and lines corresponds to Ni, the green dots and lines correspond to Cr, the red dots correspond to Fe and the lilac dots and lines correspond to Mn. The distances along the axes in Figure 1 (*a, b*) and 2 (*a*) are in Å. The right vertical axis in Figure 1 (*a*) and 2 (*a*) displays the concentration C at.% of the alloy elements.

that resistance to sliding along the grain boundaries for the studied alloys significantly increases as compared to Al. The ordered segregations of the impurity atoms at the boundaries also prevent implementation of the easiest mechanism that includes sliding and migration of the grain boundaries into Al.

In the present study, we have used the atomistic simulation methods to analyze energy characteristics of the process of sliding in the HEA CoNiCrFeMn bicrystals for the same two symmetrical grain boundaries $\Sigma5\{013\}\langle100\rangle$ and $\Sigma5\{012\}\langle100\rangle$ with a misorientation angle of $\theta = 36.87^\circ$ [12], which were previously studied by us in the Al alloys. Results for the initial state of the solid solution and after annealing are compared for the HEA alloy, wherein it is accompanied by significant concentration heterogeneity of the alloy-constituent elements near the grain boundaries. It is shown that the obtained results essentially depend on the boundary type and qualitatively differ from conclusions on the influence of the grain-boundary superstructure on resistance to sliding in the lightly doped Al alloys.

2. Simulation method

The sliding's energy barrier is calculated for the special symmetrical grain boundaries $\Sigma5\{013\}\langle100\rangle$ and $\Sigma5\{012\}\langle100\rangle$ in the CoNiCrFeMn alloy that is in the two states. The first state is a starting configuration, in which the atoms of the five sorts are randomly distributed along positions of the FCC lattice with the concentration of 20 at.% for each alloy element. The second state is a configuration of the bicrystal after annealing at $T = 723$ K using an MD/MC-procedure [8]. This state s characterized by noticeable redistribution of the atoms near the grain boundaries with formation of Cr-enriched clusters that are continuously distributed along the boundaries. We note that in both the cases a size of the simulation unit was selected to be quite large (15 lattice parameters) along the two directions in the GB plane ($\{013\}$ or $\{012\}$) in order to provide uniform distribution of the atoms along the grain boundaries.

The simulation was carried out by using the LAMMPS software package [13] and multiparticle MEAM (modified embedded-atom method) interatomic interaction potentials that are proposed in the study [14].

Figure 1 shows the fragments of the starting configurations for the grain boundaries $\Sigma5\{013\}\langle100\rangle$ (*a*) and $\Sigma5\{012\}\langle100\rangle$ (*b*). The dashed line marks sections, along which the crystallite was cut when studying sliding along the grain boundaries. It is shown in the study [8] that the structure of the grain boundary $\Sigma5\{013\}\langle100\rangle$ does not significantly change after annealing. The structural elements is slightly deformed (the structural elements are highlighted in gray in Figure 1) and the atoms are displaced from their initial positions. Figure 2 shows a region of the bicrystal near the grain boundary $\Sigma5\{012\}\langle100\rangle$, which was structurally reconstructed as a result of redistribution of the atoms near the grain boundary during MD/MC simulation.

In addition to the structural elements that correspond to the initial structure of the grain boundary $\Sigma5\{012\}\langle100\rangle$ (the two structural elements in the lower part of Figure 2, *a*), at the left and right sides of the GB starting position $X = 0$

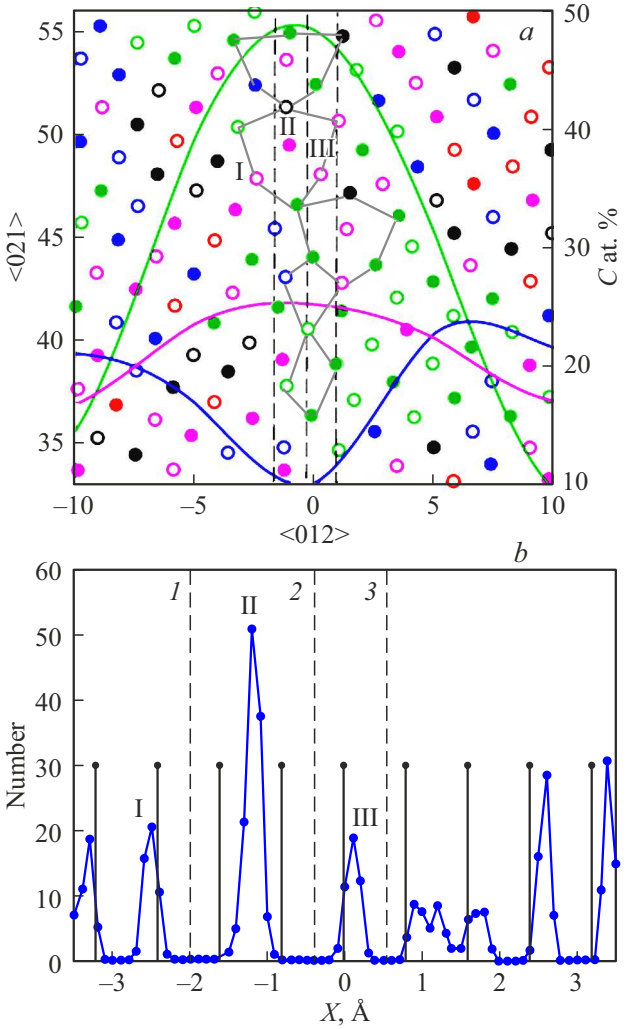

Figure 2. Fragment of the configuration of the bicrystal with the grain boundary $\Sigma5\{012\}\langle100\rangle$ (a) and the function of distribution of the atoms along the OX direction near the grain boundary (b) after 25×10^4 steps of MD/MC simulation [8]. The solid curves in Figure (b) mark the function of distribution of positions of the crystallite atoms upon completion of MD/MC simulation.

new structural elements are being formed, which are formed during boundary reconstruction. As a result, the GB width increases and the structure becomes complicated. The number of possible sections for sliding along the boundary increases (the sections I–III that are marked in Figure 2, b).

During MD/MC simulation, distribution of the atom sorts is changed near the boundaries. For both the studied grain boundaries, the Cr atoms form quite wide (of about 20 Å) segregations at the grain boundary. It is shown by analysis [8] that a width of distribution of peaks of concentration of the Cr atoms even exceeds a width of the boundary that is determined by the region near the structural elements. For the grain boundary $\Sigma5\{013\}\langle100\rangle$, the concentration of the Cr atoms can be ~ 35 at.%, and for the grain boundary $\Sigma5\{012\}\langle100\rangle$ it can be 47 at.%. The Mn atoms are also predominantly arranged near the GB center, but their concentration is much less than Cr (~ 25 at.%). The thin lines of the figures 1, 2 mark distribution of the main elements Cr, Ni, Mn that are formed in the segregation layer near the grain boundary after annealing.

In order to characterize resistance to grain-boundary shear, we have calculated the energy of a generalized stacking fault (GB-SF) or a grain-boundary γ-surface for a plane of the boundary that separates two grains. The GB-SF surface was calculated at free boundary conditions along the direction OX that is perpendicular to the GB plane and at periodic boundary conditions within the boundary plane. A certain shear vector was selected within a lattice cell **f**. One grain was sheared by this vector and the energy of the crystallite, which corresponded to the shear vector, was calculated. The energy of the surface defects was calculated as a difference between the energy of the crystallite with the stacking fault and of the crystallite without the stacking fault per a boundary area. The energy values obtained in this way form a surface of grain-boundary GB-SF shears within the lattice cell on the considered planes. Its analysis allows concluding that there are stable surface defects and determining shears that correspond to them. The crystallite was completely relaxed in points of local GB-SF minimums, while in other points that correspond to the generalized grain-boundary shear **f**, relaxation was done along the direction OX that is perpendicular to the GB plane.

3. Simulation results

For the grain boundary $\Sigma5\{013\}\langle100\rangle$, the two mutually perpendicular directions $\langle100\rangle$ and $1/2\langle013\rangle$ form the lattice cell on the plane of this boundary. Figure 3 shows the dependences of the GB-SF energy for the easiest shear directions for this boundary, which are obtained with taking into account atomic relaxation along the direction that is perpendicular to the GB plane. These shears include: along the direction along the axis of inclination of the grain boundary $\langle100\rangle$ (Figure 3, a), along the direction that is perpendicular to the inclination axis (Figure 3, b); along a broken curve through a local minimum point **A** (Figure 3, c). The shear vectors **OO1** and **OO2** are equal to translation vectors along the directions $\langle100\rangle$ and $\langle013\rangle$, respectively, and the vector **OA** is equal to $\sim 1/6\langle326\rangle$. The form of the GB-SF surfaces for the considered symmetrical grain boundaries is similar those specified in the study [11]. The value of the GB-SF energy in the point **A** is 0.53 J/m^2 for the starting configuration and 1.15 J/m^2 for the configuration after annealing. In the figures 3 and 4, the curve *1* corresponds to the starting state of the solid solution of the CoNiCrFeMn HEA, while the curve *2* corresponds to the alloy after aging at $T = 723$ K. It is clear that the curves *2* for the alloy after annealing lie higher than for the starting state of the solid solution.

The point **B** is marked on the curve *1* of Figure 3, b, c, wherein it corresponds to a local minimum, at which the

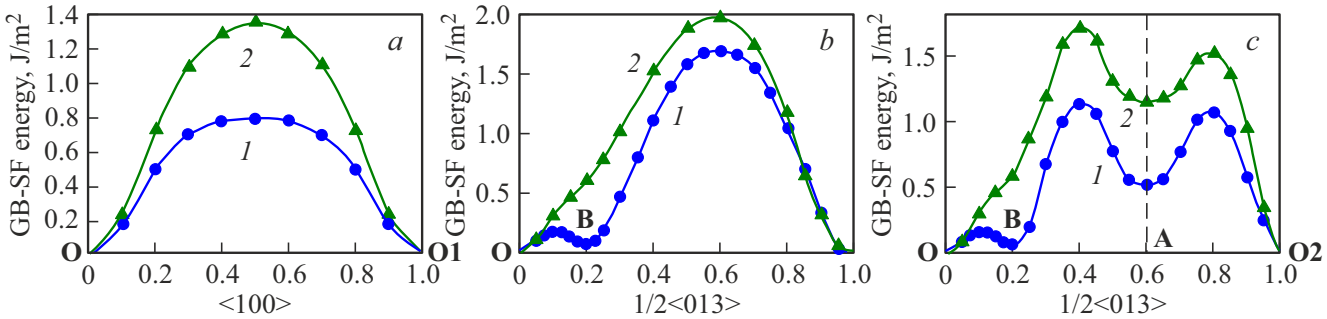

Figure 3. Variation of the GB-SF energy (with taking into account relaxation) when shearing along the direction ⟨100⟩ (*a*); along the direction ⟨013⟩ (*b*); along the combined direction OAO2 (*c*) for the grain boundary Σ5{013}⟨100⟩. The curve *1* corresponds to the solid solution, while the curve *2* corresponds to the alloy after annealing.

GB-SF energy is close to zero ($E_{\text{GB-SF}} = 0.07\,\text{J/m}^2$). The shear vector **OB** is equal to $0.2\,(1/2\,\langle 013\rangle)$ (the shear value is $0.32a$), where $a = 3.59\,\text{Å}$ is a lattice parameter. As shown in the study [11], the shear value depends only on the type of the considered grain boundary. As a result of shear **OB**, the GB plane is shifted by a value that is equal to the Burgers vector of the grain-boundary shears $\mathbf{b}_{\text{gb}}$ (see more details in the study [11]). If the chemical environment of the boundary is equivalent to the initial one, then grain boundary sliding can continue by implementing a partial shear in the next, parallel GB plane that corresponds to a new position of the grain boundary after migration. As a result of multiple repetition of the partial shear along a successive system of parallel planes, the implemented process of grain boundary sliding is accompanied by migration along a direction that is perpendicular to the GB plane. After HEA annealing, there is no local minimum near the point **B** (Figure 3). Appearance of the segregation grain-boundary layer and change of the chemical structure of the grain boundary prevent multiple grain-boundary sliding along the successive system of the parallel planes. Thus, the easiest GB-SF option for the grain boundary Σ5{013}⟨100⟩ becomes impossible.

The dependence of the energy of the surface defects on the shear value (Figure 3) can be used to derive the energy of the unstable stacking faults γ_{us} (the maximum value of the energy along the selected shear direction [3,11]). The smaller parameter γ_{us}, the more easily shearing within the GB plane along this direction during grain boundary sliding. The table shows the values of the energy of the unstable grain-boundary stacking faults with taking into account relaxation along the easiest directions of shear for HEA in the state of the solid state (the starting state) and after annealing.

It is clear from Figure 3 and the left part of the table that for all the directions of the grain-boundary shears for the grain boundary Σ5{013}⟨100⟩ the values of γ_{us} for HEA are much higher than in the starting state, i. e. appearance of the segregation layer for this grain boundary prevents sliding along the grain boundaries. It is clear from the table that the easiest direction of grain boundary sliding for the alloy in the solid-solution state is a grain-boundary partial shear **OB**, which is characterized by the value $\gamma_{\text{us}} = 0.17\,\text{J/m}^2$ that is comparable to the lowest energies of the stacking faults in the FCC-lattice metals. After annealing, the lowest one — $\gamma_{\text{us}} = 1.35\,\text{J/m}^2$ is the value for the direction of shear along the inclination axis ⟨100⟩.

The totally different situation is obtained for the grain boundary Σ5{012}⟨100⟩. The dependence of the GB-SF energy for this boundary and the values of γ_{us} for the lowest-energy directions of shear are given in Figure 4 and in the right part of the table (the vector **OO2** is equal to the shear of ⟨012⟩, **OO3** is $1/2\langle 112\rangle$). Of the three sections that are possible after annealing for this boundary (see Figure 4, *a* and Table), the lowest GB-SF values are realized for the section (sec II). For this section, all the values of γ_{us} for HEA after annealing are noticeably lower than for the alloy in the solid-solution state (Figure 4, *b*, *c*), i. e. appearance of the segregation layer for the grain boundary Σ5{012}⟨100⟩ facilitates sliding along the grain boundaries. This situation is untypical for the most segregations in the lightly doped alloys [5,6]. In the same way as previously for the grain boundary Σ5{013}, there is a partial shear **OB** with the shear vector that is equal to $0.4\langle 012\rangle$, which is related to the geometry of the grain boundary Σ5{012}⟨100⟩. For this boundary, the local minimums that correspond to the partial shear **OB** are present for the initial state of the alloy and for the state after annealing as well. The GB-SF energy for the solid-solution state is $E_{\text{GB-SF}} = 1.47\,\text{J/m}^2$ and it is $E_{\text{GB-SF}} = 1.35\,\text{J/m}^2$ for the annealed state (sec II). We note that in both the cases the energies are quite high, whereas a barrier to be overcome for GB-SF just slightly exceeds this value: $\gamma_{\text{us}} = 1.65$ and $1.36\,\text{J/m}^2$, respectively. It can be noted that the values of γ_{us} for this boundary are higher than for the grain boundaryΣ5{013} for shear along the inclination axis ⟨100⟩ as well.

4. Discussion of results

Noticeable progress has been attained in recent years in understanding the processes of interaction of the impurity atoms with the grain boundaries during annealing the binary

Energies for unstable SFes (γ_{us}, J/m^2) for the shears along the easiest directions for the grain boundary $\Sigma5\{013\}\langle100\rangle$ and the grain boundary $\Sigma5\{012\}\langle100\rangle$

GB type	$\Sigma5\{013\}$			$\Sigma5\{012\}$		
Shear γ_{us}	$\langle100\rangle$	$\langle013\rangle$	**OA-AO2**	$\langle100\rangle$	$\langle012\rangle$	$\langle112\rangle$
Starting state	0.80	0.17 (**OB**)	0.17 (**OB**)	2.04	1.47 (**OB**)	1.65–1.55
After annealing	1.35	1.96	1.71–1.52	1.77 (sec I)	1.83 (sec I)	1.83–1.75
				1.71 (sec II)	1.36 (**OB**)	1.36–1.42
				1.83 (sec III)	2.62(sec III)	2.62–2.84

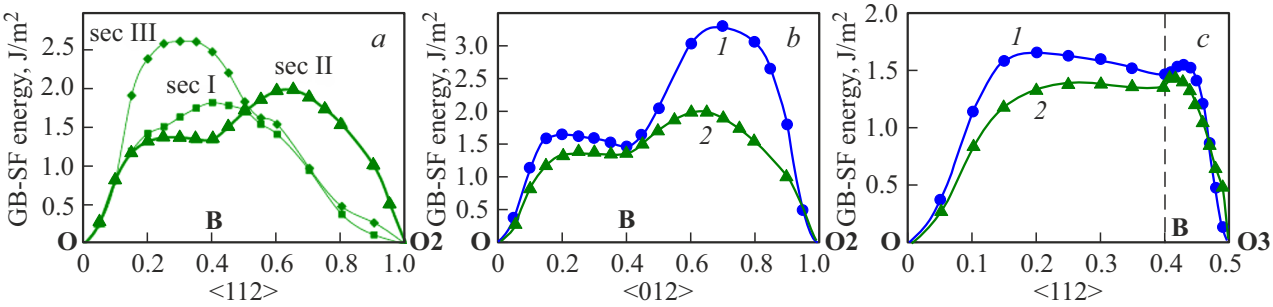

Figure 4. Variation of the GB-SF energy (with taking into account relaxation) when shearing along the direction $\langle012\rangle$ (*a, b*); along the direction $\langle112\rangle$ (*c*) for the grain boundary $\Sigma5\{012\}\langle100\rangle$. The curve *1* corresponds to the solid solution, while the curve *2* corresponds to the alloy after annealing.

lightly doped alloys [1]. However, for the lightly doped alloys not all the processes of grain boundary sliding are studied today, for example, for the grain boundaries decorated by complexones; for the alloys, in which formation of the segregations at the grain boundaries are controlled by competition between a tendency to alloy disintegration and a tendency to segregation of atoms of the doped elements [15,16].

The situation for the multi-component alloys, in particular, for HEA is even more complicated. Grain boundary sliding in the CoNiCrFeMn HEA with the FCC lattice was investigated in the present study with selecting the symmetrical grain boundaries $\Sigma5$. It enables comparing the results for HEA with the quite well-studied lightly-doped Al-based alloys [9,15]. The results of atomistic simulation of HEA in the solid-state solution were analyzed (See Figure 3, 4, Table) to show that a part of the characteristics of the sliding mechanisms qualitatively coincides with those observed in the lightly doped alloys. First of all, it is implementation of the grain-boundary partial shear **OB** that corresponds to a minimum of the GB-SF energy. This specific feature was most pronounced for the grain boundary $\Sigma5\{013\}\langle100\rangle$ (Figure 3, *b*). Both a minimum depth and a barrier height to be overcome to fall into this minimum are very low (0.07 and 0.17 J/m^2). For this grain boundary in the solid-solution state, sliding along the grain boundary is easy and comparable, in particular, to the FCC metals. For the grain boundary $\Sigma5\{012\}\langle100\rangle$, both the minimum depth and the barrier height are almost higher by an order. In general, all the values of the GB-SF energy for all the shears are higher for this grain boundary than for the grain boundary $\Sigma5\{013\}\langle100\rangle$ (see Figure 4). It can be assumed that due to a smaller volume occupied by the boundary concentration heterogeneity during distribution of the alloy atoms near the grain boundary $\Sigma5\{012\}\langle100\rangle$ results in an effect that is close to solid-solution strengthening in this region. As a result, the most favorable is the shear along the inclination axis $\langle100\rangle$ (Table). The detailed results of solid-solution strengthening during motion of twins in HEA are discussed in the studies [17–21]. The main twin braking mechanism is assumed to be elastic interaction of twinning dislocations with dissolved atoms.

Annealing and, therefore, redistribution of the alloy components near the grain boundaries differently affect the change of the sliding mechanisms for the two studied boundaries $\Sigma5$. For the grain boundary $\Sigma5\{013\}\langle100\rangle$, the GB structure is not changed significantly. It is clear from Figure 1, *a* that during formation of the grain-boundary shear the atoms near a selected section are moved into the region with a significant gradient of concentration of the main elements Cr, Mn, Ni, which segregate at the grain boundary during annealing. Chemical interaction of the atoms near the section is changed and local concentration heterogeneity increases. It is calculated to show that this influence results in disappearance of implementability of the grain-boundary partial shear **OB**; that the values of

the GB-SF energy increase as a whole; and that the most favorable is the shear along the inclination axis $\langle 100 \rangle$ (see Figure 3, *b*, Table). All these changes are significantly equivalent to the influence of segregations in the lightly doped alloys on grain-boundary mobility [11].

The different situation is obtained for the grain boundary $\Sigma 5\{012\}\langle 100 \rangle$. The values of the GB-SF energy for all the grain-boundary shears are essentially reduced as compared to the solid-solution state (Figure 4, Table). The grain-boundary partial shear OB is preserved and becomes the most favorable, while the barrier (γ_{us}) for formation of this partial shear is reduced, too. By external features, the state of the alloy in the region near the grain boundary is close to a pure-metal state with strengthening that may be solid-solution one. As shown in the study [8], after annealing the CoNiCrFeMn HEA exhibits a pronounced tendency to formation of predominantly Cr segregations at the grain boundaries. The width of the concentration peak for $\Sigma 5\{012\}\langle 100 \rangle$ can be ~ 20 Å, while the peak height can be 47 at.%, wherein the maximum value of the Cr concentration falls on sec II, for which the above-described specific features of grain-boundary sliding are obtained (Figure 2, *a*). It can be noted that the width of the grain boundary (a size of the structural element along a direction perpendicular to the boundary plane) is less than the region of a noticeable change of concentration of the segregating atoms. The grain boundary $\Sigma 5\{012\}\langle 100 \rangle$ differs from $\Sigma 5\{013\}\langle 100 \rangle$ in this respect. For the other sections $\Sigma 5\{012\}\langle 100 \rangle$ (sec I, sec III, see Figure 3, *b*), where on average the Cr concentration is much lower, the influence of the segregations is similar to the lightly doped alloys (Figure 4, *a*, Table). Thus, presence of the high concentration of the same-sort atoms in a band that determines the structure of the grain boundary and its position can result in implementation of the sliding mechanisms that are typical for pure metals. A decrease or increase of resistance to sliding will be determined by the type of the grain boundary and the type of the segregated atoms. It can be assumed that a similar situation can be implemented for the multi-layer complexones [1–3] or for other cases of wide distribution of the impurity atoms near the grain boundary [4].

It is shown in the experimental studies [17–21] that grain refinement of the single-phase CoNiCrFeMn HEAs to the size ~ 100 nm can significantly increase their strength, thereby indicating an important contribution by the grain-boundary mechanisms of strengthening. Usually, grains are refined as a result of thermal-mechanical treatment. Our results show that the processes of strengthening and sliding along the grain boundaries substantially depend on a nature of development of the segregation processes. Distribution by types of the grains realized in the ensemble can be significantly changed during redistribution of the alloy components. At the same time, an HEA concentration composition can be significantly changed inside the grain, thereby affecting a mutual dependence of intragranular deformation of the alloy and deformation along the grain boundaries. It should be noted that the above-discussed GB migration processes are implemented for the specific case of the symmetrical special grain boundaries of the inclination. In a fine-grained polycrystal with predominance of arbitrary grain boundaries, the stress-induced boundary-migration mechanism can be more complex and can include processes that provide sliding of the non-symmetrical grain boundaries by motion of steps [19] and deformation compatibility in the triple junctions of the grains [20].

Nevertheless, the results obtained in the present study give an idea of fundamental mechanisms that determine grain sliding and of conditions of implementation of the stress-induced grain-boundary-migration mechanism in the CoNiCrFeMn HEA.

5. Conclusions

In order to clarify the specific features of grain boundary sliding in HEA, we have carried out atomistic simulation of the CoNiCrFeMn alloy that has special grain boundaries of the inclination $\Sigma 5$. The obtained results suggest the following conclusions.

1. It is shown that in the solid-solution state with homogeneous distribution of the five components the CoNiCrFeMn HEA behaves during grain boundary sliding qualitatively similarly to the pure FCC metal, including implementation of the easiest mechanism of sliding and migration along the grain boundaries.

2. It is shown that appearance of the segregation layer of the Cr atoms during annealing facilitates sliding along the grain boundaries for the grain boundary $\Sigma 5\{012\}\langle 100 \rangle$, whereas sliding is hindered for the grain boundary $\Sigma 5\{013\}\langle 100 \rangle$. Despite a pronounced tendency to formation of the segregations at the grain boundaries, the behavior of the grain boundary during grain boundary sliding retains features of the homogeneous solid solution $\Sigma 5\{012\}\langle 100 \rangle$.

3. Due to substantial redistribution of the alloy components, the multidirectional effect of thermal-mechanical treatment on the grain boundaries of the different type can significantly affect the structure of the ensemble of the HEA grain boundaries and its stability.

Funding

The study was conducted under the state assignment of the Ministry of Education and Science of the Russian Federation for the Institute of Metal Physics, Ural Branch of the Russian Academy of Sciences

Conflict of interest

The authors declare no conflict of interest.

References

[1] Ch. Hu, R. Dingreville, B.L. Boyce. Comp. Mat. Sci. **232**, 112596 (2024).
[2] P. Lejček. Grain Boundary Segregation in Metals, Vol. **136**, Springer Science & Business Media, (2010)
[3] P.R. Cantwell, M. Tang, S.J. Dillon, J. Luo, G.S. Rohrer, M.P. Harmer. Acta Mater. **62**, 1–48 (2014)
[4] L.E.Karkina, I.N.Karkin, A.R. Kuznetsov, I.K. Razumov, P.A. Korzhavyi, Yu.N. Gornostyrev. Comp. Mat. Sci. **112**, 18 (2016).
[5] L.Karkina, I. Karkin, A.Kusnetsov, Yu.Gornostyrev. Metals. **9** (12), 1319 (2019).
[6] A. Kuznetsov, L. Karkina, Yu. Gornostyrev, P. Korzhavyi. Metals. **11**. 631 (2021).
[7] L.E. Kar'kina, I.N. Kar'kin, Yu.N. Gornostyrev. FMM. **124**, 971 (2023). (in Russian).
[8] L.E. Kar'kina, I.N. Kar'kin, Yu.N. Gornostyrev. FMM. **126**, 38 (2025). (in Russian).
[9] L.E. Kar'kina, I.N. Kar'kin, Yu.N. Gornostyrev. FMM. **121**, 901 (2020). (in Russian).
[10] L.E. Kar'kina, I.N. Kar'kin, Yu.N. Gornostyrev. FMM. **122**. 1187 (2021). (in Russian).
[11] L.E. Kar'kina, I.N. Kar'kin, A.R. Kuznetsov, Yu.N. Gornostyrev. FTT. **60**, 1974 (2018). (in Russian).
[12] R.Z. Valiev, A.N. Vergazov, V.Yu. Gertsman. Kristallogeometricheskii analiz mezhkristallitnykh granits. Nauka, M. (1991). 231 s. (in Russian).
[13] http://lammps.sandia.gov/index.html.
[14] W.M. Choi, Y. Kim, D. Seol, B.J. Lee. Comp. Mater. Sci. **130**, 121 (2017).
[15] I.N. Karkin, L.E. Karkina, A.R. Kuznetsov, M.V. Petrik, Yu.N. Gornostyrev, P.A. Korzhavyi. Mater. Phys. Mech. **24**. 201 (2015).
[16] I.N. Kar'kin, L.E. Kar'kina, P.A. Korzhavyi, Yu.N. Gornstyrev. FTT, **59**. 103 (2017). (in Russian).
[17] H. Shahmir, T. Mousavi, J.Y. He, Z.P. Lu, M. Kawasaki, T.G. Langdon. Mater. Sci. Eng. A **705**, 411 (2017).
[18] N.D. Stepanov, D.G. Shaysultanov, R.S. Chernichenko, N.Y. Yurchenko, S.V. Zherebtsov, M.A. Tikhonovsky, G.A. Salishchev. J. Alloy. Compd. **693**. 394 (2017).
[19] R. Hadian, B. Grabowski, C.P. Race, J. Neugebauer. Phys. Rev. B. **94**. 165413 (2016).
[20] M.Yu. Gutkin, K.N. Mikaelyan, I.A. Ovid'ko. Phys. Sol. State. **50**. 1266 (2008).
[21] R.E. Kubilay, W.A. Curtin. Acta Materialia. **216**, 117119 (2021).

Translated by M.Shevelev